Journal of Nano Research
ISSN: 1661-9897, Vol. 85, pp 43-52
doi:10.4028/p-M2jprp

Submitted: 2024-01-24
Revised: 2024-04-19
Accepted: 2024-04-30
Online: 2024-11-29

Synthesis, Dynamic Mechanical Properties of Poly(Styrene-co-Acrylonitrile) Grafting Silica Nanocomposites

Moussa Khlifa[1,a*], Wanisa Abdussalam-Mohammed[2,b] Ahmed Zaed[3,c], Valeria Arrighi[4,d] and Arno Kraft[4,e]

[1]Chemistry Department, Faculty of Science, Sebha University, Libya

[2]Chemical Engineering, Faculty of Engineering, Tripoli University, Libya

[3]Chemistry Department, Faculty of Science ,Derna University, Libya

[4]Institute of Chemical Sciences, Heriot Watt University, UK

[a*]Mou.Khlifa@gmail.com, [b]w.ahweelat@uot.edu.ly, [c]ahmed70_07@yahoo.com, [d]V.arrighi@hw.ac.uk, [e] A.kraft@hw.ac.uk

*Corresponding author: Mou.Khlifa72 @ gmail.com

Keywords: Silica Nanoparticles, ATRP , PSAN, Reinforcement.

Abstract. A series of styrene–acrylonitrile (SAN) copolymer nanoparticles were prepared by grafting styrene–acrylonitrile from both aggregated silica and colloidally dispersed silica nanoparticles using atom-transfer radical polymerisation (ATRP). Cross-linking and macroscopic gelation were minimised by using a miniemulsion system. The thermal and mechanical behavior of composites were made from PSAN aggregated silica nanoparticles or colloidally dispersed silica has been examined by Differential scanning calorimetry (DSC) and Dynamic mechanical thermal analysis (DMTA). The filler particles increased the rubbery modulus above the T_g of PSAN considerably and led to a temperature-independent plateau of the modulus between 130 and 240 °C similar to that normally observed for crosslinked amorphous polymers. Covalent attachment of PSAN to the silica nanoparticles, by grafting the polymer from the surface of the silica using atom-transfer radical polymerization (ATRP), gave rise to hybrid materials with a comparable elastic plateau. While neat PSAN started to flow and deform irreversibly above 120 °C, the new silica nanoparticle–polymer hybrid materials proved stable up to 240 °C, which was more than 120 °C above the T_g of the polymer. Aggregated silica nanoparticles displayed more affect compared to colloidally dispersed silica.

1. Introduction

For polymeric systems, improved mechanical behavior is traditionally achieved by the addition of fillers such as carbon black, clays, talc and silica. These composites have been widely studied and owe their success to their strength, light weight and low cost.

The nature of the reinforcement effect in polymer–filler composites has been extensively discussed in the literature. It is known that polymer–particle as well as particle–particle interactions play a very important role in determing the reinforcing ability of a composite. Particle pre-treatment is often a necessary step used to improve polymer–particle interactions and experimental results have demonstrated improved mechanical behavior at low filler content [1,2]. At high filler concentration, particle–particle aggregation may dominate the mechanical response with a consequent decrease in the level of improvement. Controlling the dispersion of fillers in a polymer matrix is crucial but not always straightforward : poorly bonded particles increase brittleness and lower the composite's resistance to crack growth [3]. Nanosize inorganic particles affect larger improvements in mechanical properties compared to micron-sized fillers. Two recent developments have renewed the interest in cheap silica fillers. First, silica nanoparticles are commercially available and their high surface–to–volume ratio promises excellent compatibility with many polymer matrices. Second, new controlled radical polymerization techniques have emerged for grafting polymers from the surface of silica and other nanoparticles which allow polymer and filler particle to become intimately linked to each other.

Rühe first reported the attachment of polymers to silica nanoparticles using a surface-grafted azo initiator and a conventional radical polymerization [4,5]. More recently, controlled radical polymerizations have been used to generate surface-grafted polymer chains. The general strategy involves the covalent linking of a suitable initiator onto the silica surface, followed by controlled radical polymerization of a vinyl monomer. Contributions from termination reactions that are typical for conventional radical processes become, if not negligible, at least minimized in controlled radical polymerizations as the concentration of active radical species is considerably reduced. This allows well-defined polymers to be synthesized with narrow molar mass distributions (M_w/M_n < 1.3) and predetermined degrees of polymerization (DP = [monomer]/[initiator]). Atom-transfer radical polymerization (ATRP) has been successful in controlling molecular weight and polydispersity of various surface-grafted polymers, such as polystyrene and poly(methyl methacrylate)[6-13]. and even block copolymers [6-11]. In contrast, nitroxide-mediated polymerization and reversible addition fragmentation chain transfer (RAFT) polymerization seem to be more restricted with regard to the choice of monomer and require a more elaborate synthesis for the surface initiating group [12-14]. Despite their potential wide-ranging engineering applications, very little is known about the effect of surface-grafted filler particles on the mechanical and thermal properties of the resulting nanocomposites. Most mechanical studies have dealt with either unmodified nanosilica or commercially available surface-modified particles [15-16].

In this paper, we reported the synthesis of Poly(styrene-co-acrylonitrile) (PSAN), chains from aggregated silica nanoparticles or colloidally dispersed silica by ATRP in miniemulsion as well as our results on the thermal and dynamic mechanical properties of these hybrid. Reactive silica particles have already been converted into PSAN composites [17-19]. These studies were carried out by dispersing non-aggreggating spherical silica nanoparticles, which were either untreated or surface-modified, in styrene and acrylonitrile monomers, followed by polymerization using a free radical initiator. Although chemical bonds between organic and inorganic phase are likely to exist in such cases, the free radical polymerization process also produces free polymer chains, unattached to the silica surface. This is therefore different from the grafting process described here.

To be able to compare the properties of PSAN–grafted particles to those of more conventional PSAN/nanosilica composites, we prepared also a series of samples by dispersing silica nanoparticles in a tetrahydrofuran (THF) solution of PSAN and investigated their mechanical behavior using dynamic mechanical thermal analysis (DMTA).

2. Material and Methods

2.1 Reagents

Commercial PSAN (25.6 wt% AN) used in dispersed nanocomposites was provided by Sigma-Aldrich, ascorbic acid and triethylamine from Lancaster; styrene (>99%), acrylonitrile (>995), copper(II) chloride (+99%), 3 aminopropyltriethoxysilane, anisole, tin(II) 2-ethylhexanoate ($Sn(EH)_2$), N,N,N',N",N"-pentamethyldiethylenetriamine (PMDETA), and hexadecane from Aldrich. Hydrophilic Cab-o-sil H5 silica particles with a specific surface area of 300±30 m^2/g and a diameter of 7 nm were obtained from Cabot and a 30% solution MEK-ST Colloidal silica, having a particle size between 10-15 nm from Nissan Chemical.

2.2 Preparation of O-2,2,2-Trichloroethyl N-(3-Triethoxysilylpropyl)carbamate (Trichloroethyl Carbamate Initiator). A mixture of 3-aminopropyltriethoxysilane (13.6 mL, 12.9 g, 58.4 mmol), 2,2,2-trichloroethyl chloroformate (7.9 mL, 12 g, 58 mmol), and triethylamine (10.0 mL, 7.26 g, 71.7 mmol) in toluene (100 mL) was stirred at 40 °C for 4 hours. The reaction mixture was filtered to remove triethylammonium chloride. The filtrate was concentrated in vacuum to give a yellow-brown oil (20.6 g, 89%). For analysis, the crude product was further purified by vacuum distillation (Kugelrohr, 205 °C/0.4 mbar) to yield ATRP initiator **1** as a colorless liquid.

^{1}H NMR (200 MHz, $CDCl_3$): δ 0.64 (t, J = 7.9 Hz, 2 H), 1.22 (t, J = 7.1 Hz, 9 H), 1.67 (tt, J = 7.9, 6.6 Hz, 2 H), 3.24 (q, J = 6.6 Hz, 2 H), 3.82 (q, J = 7.1 Hz, 6 H), 4.71 (s, 2 H), 5.38 (br. t, 1 H). ^{13}C NMR (50 MHz, $CDCl_3$): δ 7.52 (CH_2), 18.16 (CH_3), 22.88 (CH_2), 43.47 (CH_2), 58.35 (CH_2), 74.29 (CH_2), 95.62 (C), 154.47 (C). IR (KBr, cm^{-1}): □ 3338 (bs), 2974 (s), 1733 (s), 1538 (s), 958 (s). MS

(CI, NH_3): m/z 417, 415, 413 (1, 3, 3%), 352, 350 (9, 10), 265 (27), 222 (100), 208 (25), 176 (33). Exact mass calcd. for $C_{12}H_{24}{}^{35}Cl_3NO_5Si + NH_4^+$ requires m/z 413.0828, found 413.0826 (CI, NH_3). Anal. Calcd. for $C_{12}H_{24}Cl_3NO_5Si$ (396.8): C, 36.33; H, 6.10; N, 3.53. Found: C, 35.88; H, 5.72; N, 3.53.

2.3 Synthesis of Trichloroethyl Carbamate-Functionalized Silica Nanoparticles. Silica nanoparticles were dried at 110 °C/0.03 mbar for 6 hours. A slurry of silica nanoparticles (5.1 g), trichloroethyl carbamate initiator **1** (273 mg, 0.688 mmol), and toluene (90 mL) was heated to 110 °C for 12 hours. The solid was centrifuged (4000 rpm, 20 min) and the supernatant decanted. Centrifugation–decantation was repeated 3 times with THF as the extracting solvent. The gel layer was transferred into a pre-weighed beaker and dried in an oven at 60 °C overnight.

2.4 Synthesis of Tris(2-dimethylamino)$_{ethyl}$)amine(Me_6TREN)

The synthesis of Me_6TREN was carried out according to a previously reported method[20]. A mixture of 13mL formaldehyde (37 w/w) and 15.4 mL of formic acid (90% w/w) was stirred at 0 ºC for 1 hour. To this mixture a solution of tris(2-aminoethyl)amine (4.22 g, 29 mmol) and 2.5 mL deionised water was added drop-wise. The mixture was gently refluxed overnight at 100 ºC. After cooling to room temperature, the volatiles were removed by rotary evaporation. The residue was treated with a saturated sodium hydroxide aqueous solution (30 mL). Then the oily layer was extracted into ether.

The organic phase was dried over anhydrous sodium sulphate and the solvent was removed by rotary evaporation to produce a slightly brown oil product. Yield (65%). For analysis, the crude product was further purified by vacuum distillation (Kugelrohr, 230 °C/0.4 mbar). ^{1}H NMR (300 MHz, $CDCl_3$): δ 2.21(s, 18H), 2.32 (dd, 12H), 2.55 (dd, 12H). Anal. Calcd. For $C_{12}H_{30}N_4$ (230.39): C, 62.56; H, 13.12; N, 24.32. Found: C, 62.64; H, 13.32; N, 24.21.

2.5 ATRP of SAN from Trichloroethyl Carbamate-Functionalized Silica Nanoparticles in Miniemulsion Initiator modified silica nanoparticles (0.20 g, 18.8 μmol; 0.047) were dispersed in anisole (6 mL) with stirring for 12 hours in a Schlenk flask. Styrene (2.44 mL, 21.3 mmol) and acrylonitrile (0.82 mL, 12.5 mmol) were added, and then a solution of $CuCl_2$ (0.21 mg, 0.94 μmol), Me_6TREN (0.390 μL, 0.94 μL) complex in anisole (0.75 mL) was added. The mixture was degassed by three freeze-pump thaw cycles. A solution of $Sn(EH)_2$ (5.00 μL, 15.41 μmol) and Me_6TREN (6.50 μL, 15.4 μmol) in anisole (0.5 mL) was added. The Schlenk flask was then transferred into a thermostatic oil bath at 90ºC. The reaction was stopped after 50 hours by exposing the catalyst to air. The product was precipitated into methanol (700 mL) over 30 minutes then the supernatant removed by filtration. The precipitated was dried in a vacuum oven at 60 ºC.

2.6 Preparation of Silica-Filled PSAN by Solution Dispersion. A 5% solution of PSAN in THF along with the required amount of silica particles were added to a flask. The flask was sealed to prevent evaporation and the slurry was stirred for 48 hours. After evaporation of the solvent at room temperature, the residue was dried in an oven at 160 °C for 24 hours.

2.7 Cleavage of PSAN from Silica–PMMA Hybrid Nanoparticles. A procedure similar to that described by Antoni et al. [21]. was used for cleaving polymer chains from functionalized silica nanoparticles. Silica–PSAN hybrid particles (0.3 g) were suspended in THF (15 mL) and a 1 M solution of tetrabutylammonium fluoride in THF (1.5 mL) was added. The mixture was then stirred for 3 days. After centrifugation (4000 rpm, 20 min), the supernatant was decanted and poured into hexane. The precipitate was collected by suction filtration and dried in an oven at 75 °C.

2.8 Characterization. ^{1}H NMR spectra were recorded on a Bruker AC 200. Infrared spectra were obtained with a Perkin Elmer RX Fourier transform infrared spectrometer, and CHN analyses were performed on an Exeter CE-440 Elemental Analyzer. Average molar masses, M_w and M_n, as well as molar mass distributions were determined by gel-permeation chromatography (GPC) using a Polymer Labs PL-GPC50 equipped with a differential refractometer (calibrated with PMMA standards; elution solvent: THF; flow rate: 1.0 mL min^{-1}; temperature: 35 °C). Differential scanning calorimetry (DSC) analyses were performed with a Thermal Advantage DSC 2010 at a heating rate of 20 °C min^{-1} under a constant nitrogen flow. Glass transition temperatures were taken as the mid-

point of the transition. Dynamic mechanical analysis measurements were carried out in cantilever mode with a TA Instruments DMA 2980 at a frequency of 1 Hz and a heating rate of 2 °C min^{-1}. Samples were prepared from silica–PSAN hybrid particles (ca. 0.3 – 0.4 g) in a rectangular steel mold using a hot press (set to 200 °C while applying a weight of 5000 tons for 40 min). Thermogravimetric analyses were carried out with a Dupont Instruments 951 Thermal Analyzer. Approximately 14 mg of silica–PSAN hybrid particles were heated under a flow of dry nitrogen at a heating rate of 7.5 °C min^{-1} over a temperature range of 40 – 815 °C. The microstructures of the prepared polymer composites, after coating samples with a thin film of gold, were examined using a FEI Instruments Quanta 3D FEG Scanning electron microscope (SEM).The TEM experiments were done using a FEI Tecnai F20-G2 operated at 200 kV. The modified silica nanoparticles were dispersed in toluene (10 mg in 3 mL) for 24 hours at room temperature. These dilute solutions were cast onto carbon-coated copper grids film and analyzed after evaporation of the solvent.

3. Results and Discussion

3.1 Synthesis and Characterization of Grafted-PSAN/Silica Nanocomposites

The synthetic strategy for the preparation of PSAN-grafted silica nanoparticles is outlined in Scheme 1. Following a report on the suitability of trichloromethyl (CCl_3) groups as ATRP initiators[22-23], we synthesised the new ATRP initiator **1** in a one-step process from commercially available and an expensive compounds 3-aminopropyltriethoxysilane and trichloroethyl chloroformate. Although the trichloroethyl group is primary considered in Organic Chemistry to be a protecting group for amines, thiols and alcohols, abstraction of a single chlorine by a suitable Cu(I) catalyst is possible and will initiate the controlled radical polymerisation. The use of a triethoxysilane group provides up to three sites for attachment to silica. In addition, the reaction with triethoxysilane group forms a stable Si-O-Si bond via a condensation reaction [24]. Initially, ATRP in miniemulsion was attempted with a mixture of styrene and acrylonitrile However, mini-emulsion is carried out in water, and acrylonitrile is relatively soluble in water[25] Thus water was replaced with anisole as shown in the literature[26], keeping the styrene and acrylonitrile mixed together so that polymerisation can take place. The monomer feed was close to the azeotropic composition (ca. 63 mol% styrene and 37 mol% acrylonitrile), and copolymerisation was conducted in the presence of catalyst system in anisole as described in Scheme 1. ATRP was conducted with 2-bromoisobutyryl amide or trichloroethyl-carbamate functionalised silica as initiators, Me_6TREN/Cu(II) as the catalyst, and an organic-soluble tin salt for reducing Cu(II) to Cu(I) instead of ascorbic acid in anisole at 90 °C. The reason for using tin(II) 2-ethylhexanoate ($Sn(EH)_2$) is because ascorbic acid is not soluble in anisole. $Sn(EH)_2$ was successfully used as the reducing agent in ATRP polymerisation, with different monomers such as butyl acrylate, styrene, methyl methacrylate and acrylonitrile [27-28]. The amounts of catalyst were varied to define the optimum conditions for control of SAN polymerisations. Three different amounts of Cu(II) were used 0.50, 1.00, and 2.00 equiv vs. $Sn(EH)_2$. An organic reducing agent, glucose, was also examined for the ATRP of SAN to reduce the absolute amount of any metals in an ATRP process. Glucose has the advantage that it is soluble in polar solvents and environmentally benign. However, using glucose as reducing agent no polymerisation of SAN was observed. This result could be due to the added amount of glucose not being enough to initiate the polymerisation. The polymerisation was finished by opening the flask and exposing the catalyst to air after 50 h. The product was further purified by extensive Soxhlet extraction with THF to remove free, unattached polymer. The amount of covalently attached PSAN from elemental analysis was in the range of 78 to 90 wt%, corresponding to a silica content of 10 – 22 wt%. Elemental analyses data were found to be in agreement with TGA measurements, as shown in Figure 1 for one of the silica–PSAN

Furthermore, selective TEM and SEM images of grafted PSAN silica particles are shown in Figure 2. The TEM and SEM images clearly demonstrates that a good dispersion of particles in the polymer matrix was observed. Values of average molar mass were obtained by GPC, after cleaving the polymer chains from the silica surface using tetrabutylammonium fluoride, and are reported in Table 1. The molar mass was slightly higher and molar mass distribution relatively broader than expected for AGET ATRP polymersiation, with polydispersites of 1.7 − 2.3. The high PDI can be attributed to very small amount of Cu(II) and relatively slow the deactivation[29].

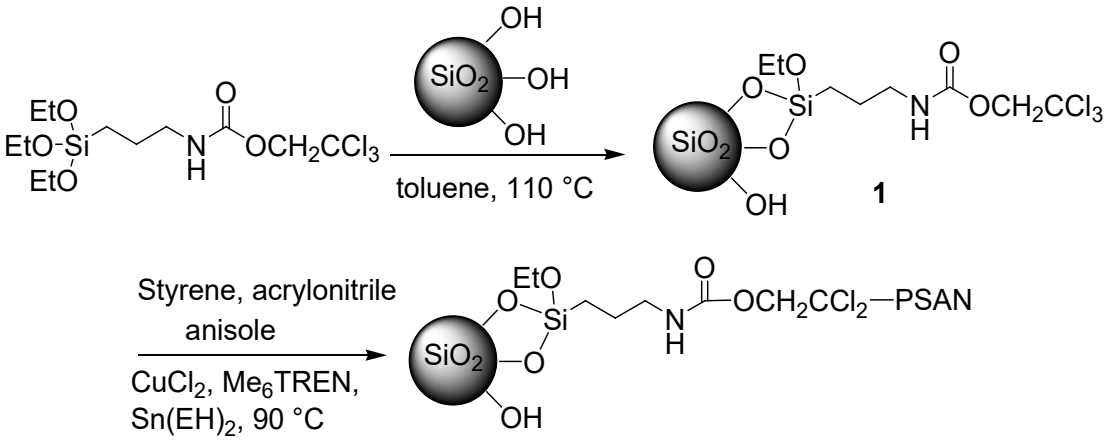

Scheme 1. Synthetic scheme for the grafting of PSAN from silica nanoparticles using ATRP

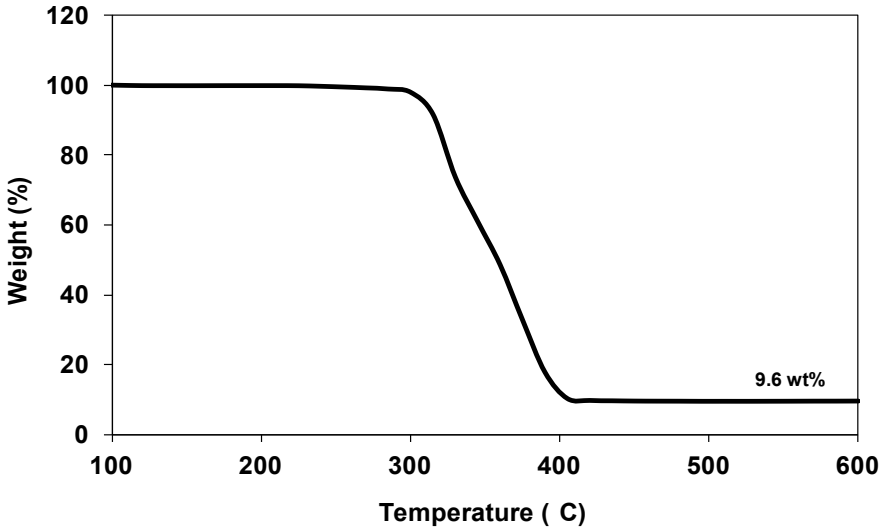

Fig. 1. TGA analysis of a grafted-PSAN/silica nanocomposite (G190-9.5Si).

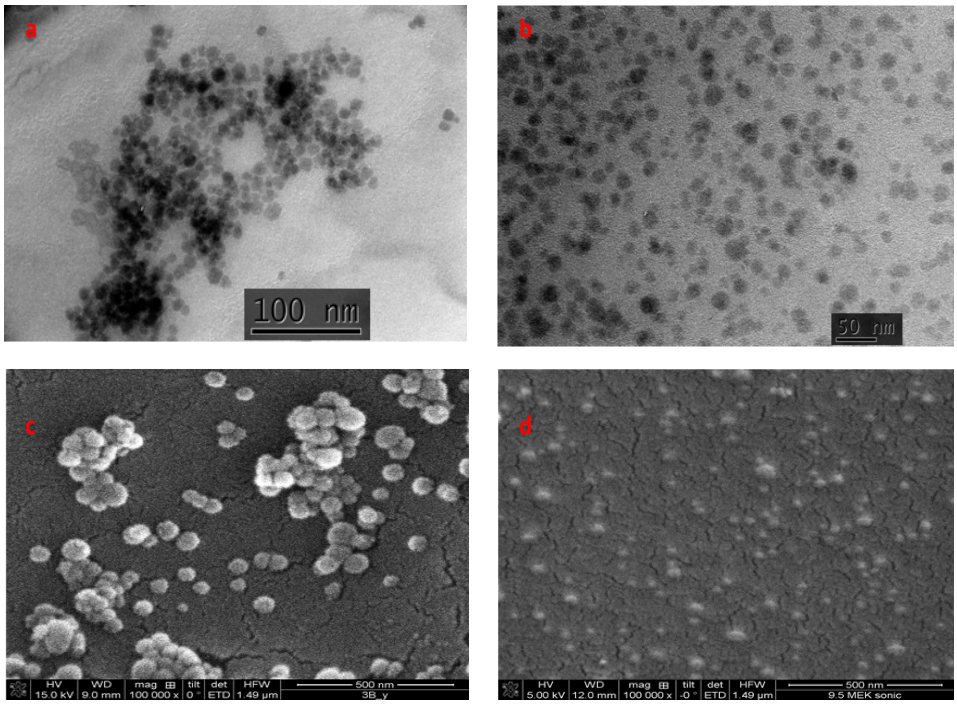

Fig. 2. a) TEM of G140-18Si; b) TEM of G139-12.7Si; c) SEM of G140-18Si and d) SEM of G139-12.7Si

Table 1. Characteristics of PSAN-grafted SiO_2 Particles

Sample code	% SiO_2	M_w [c)] [g mol^{-1}]	PDI	T_{max} (tan δ) °C	T_g [d)] °C
PSAN	0.0	110000		114	107
G190-9.5Si [a)]	9.5	190000	1.83	116	112
G139-12.7Si [a)]	12.7	139000	2.31	122	114
G184-12.8Si [b)]	12.8	184000	1.76	115	115
G140-18.3Si [b)]	18.3	140000	2.22	118	111
Error	-----	--------		±1	±1

[a)] PSAN-MEK-ST. "G190" refers to a molecular weight of 190 kg mol^{-1} for the grafted PSAN, "9.5Si" stands for a silica 9.5 wt%. [b)]PSAN-Cab-o-sil H5. [C)] calculated by GPC. [d)]calculated by DSC

3.2 DMTA Analysis of Grafted/ Dispersed PSAN Silica Nanocomposites

All samples were thoroughly dried at 160 °C since the T_g of PSAN was sensitive to the presence of plasticizing solvents. As illustrated in Table 1, the glass transition temperatures measured by DSC are usually higher for the hybrid material compared to pure PSAN. Similar conclusions can be drawn by considering the temperatures corresponding to tan δ maximum (Table 1). The T_g increase observed for the grafted systems compared to PSAN(at most 8 degrees for **G184-12.8Si**) seems to be dependent on the molecular weight of the grafted chains as well as nanosilica content.

Figures 3 and **4** show the DMTA data (E′, and tan δ) for the grafted PSAN samples prepared in this project. The normalised E′ versus temperature curves once again reveal a pronounced reinforcement effect at temperatures above the glass transition. Similar to the polymer–silica mixtures studied before, the modulus of the hybrid materials containing 9.5 and 18.3% silica remained almost constant above T_g, until up to 240 °C and did not show the irreversible deformation that unfilled PSAN exhibits above 120 °C. The reinforcing effect on the modulus is not unusual and comparable to composites of single-walled carbon nanotubes in styrene–isoprene copolymers [30], which also possessed a rubbery plateau that extended to over 250 °C. The grafted non-aggregated silica nanoparticles samples (**G190-9.5Si** and **G139-12.7Si**) show a slightly higher storage modulus than pure PSAN before the onset of deformation; however it is the grafted aggregated silica (**G140-18.3Si)** that exhibits the greatest increase in storage modulus in the rubbery region.

In addition, the tan δ vs. temperature plots, **Figure 3**, show broadening with increasing of silica content. This behaviour is similar to that observed earlier in literature[23]. As compared to the dispersed composites, grafted PSAN/silica samples display a higher storage modulus above the T_g and suppress sample deformation up to 240 °C, more than 130 °C above the glass transition of neat PSAN. Unlike dispersions of silica in PASN, the hybrid particles exhibited little mechanical damping at high temperature as evidenced by a surprisingly low tan δ (<0.1) throughout the plateau region of the modulus. Furthermore, the hybrid material exhibited little signs of degradation or irreversible deformation. The low tan δ values measured for the grafted-PSAN/silica nanocomposites suggest the mechanical response above the glass transition to be elastic. All four tan δ curves provide clear evidence for the suppression of the terminal flow region, a result that is similar to that expected for single-phase, cross-linked amorphous materials [31].

A direct comparison of the E′ vs temperature curves of dispersed and grafted samples with comparable silica content (**Figure 5**) shows that, while there are clear differences in the glass transition region (in terms of its location, width of the relaxation process). It is apparent from **Figure 5** that the grafted composites have a higher storage modulus above the glass transition and suppressed sample deformation compared to pure PSAN or dispersed samples. Furthermore, the DMTA data of grafted composites could be collected up to 250 °C, more than 130 °C above the T_g of pure PSAN. Storage modulus values at high temperature are close for Cab-o-sil H5 samples having similar wt% silica. This leads us to conclude that the reinforcement effect is largely determined by the 3-dimensional network structure of polymer and filler, and therefore related to the silica content.

Colloidally dispersed silica nanoparticles (MEK-ST) gave rise to only a marginal improvement in modulus compared to grafted Cab-o-sil H5. Thus, for this system grafting has little impact on the extent of reinforcement but, in suppressing chain diffusion and flow, it appears to extend the region over which rubbery behavior is observed, without a need for cross-linking.

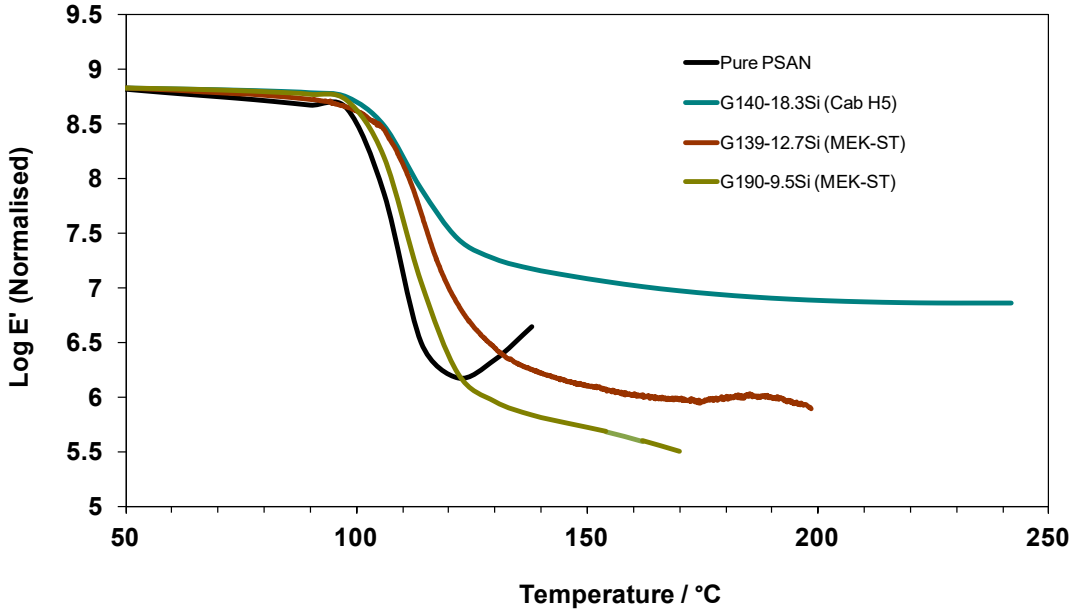

Fig. 3. Plot of normalised storage modulus as a function of temperature for pure PSAN and grafted PSAN-silica nanoparticles prepared from MEK-ST and Cab-o-sil H5 (percentage of silica, as indicated).

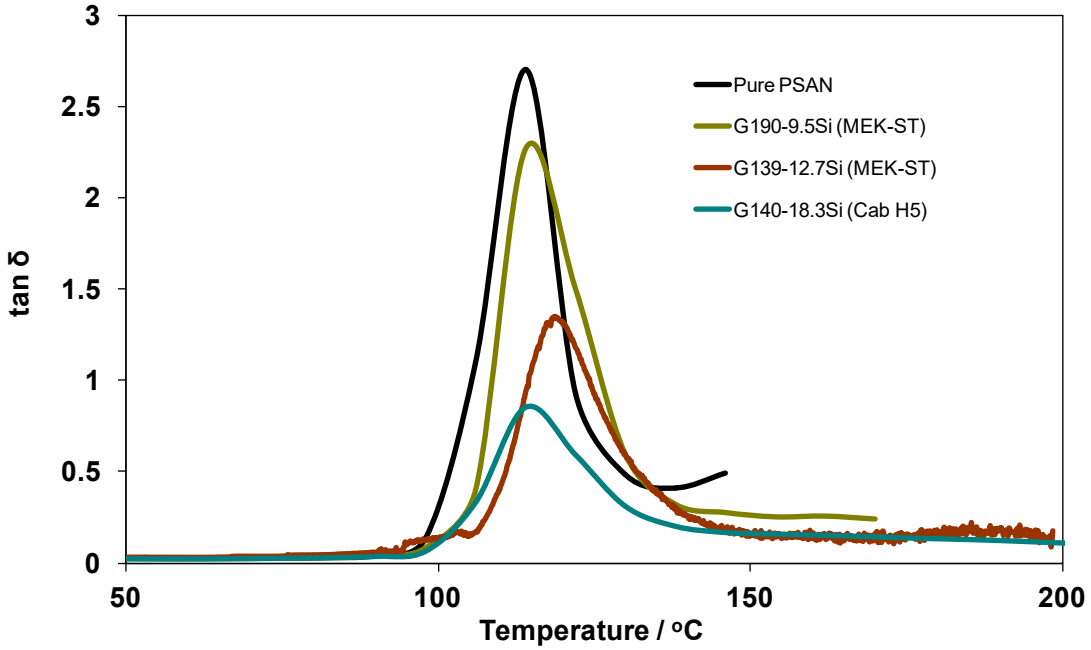

Fig. 4. Plot of tan δ as a function of temperature for pure PSAN and grafted PSAN-silica nanoparticles prepared from MEK-ST and Cab-o-sil H5 (percentage of silica, as indicated).

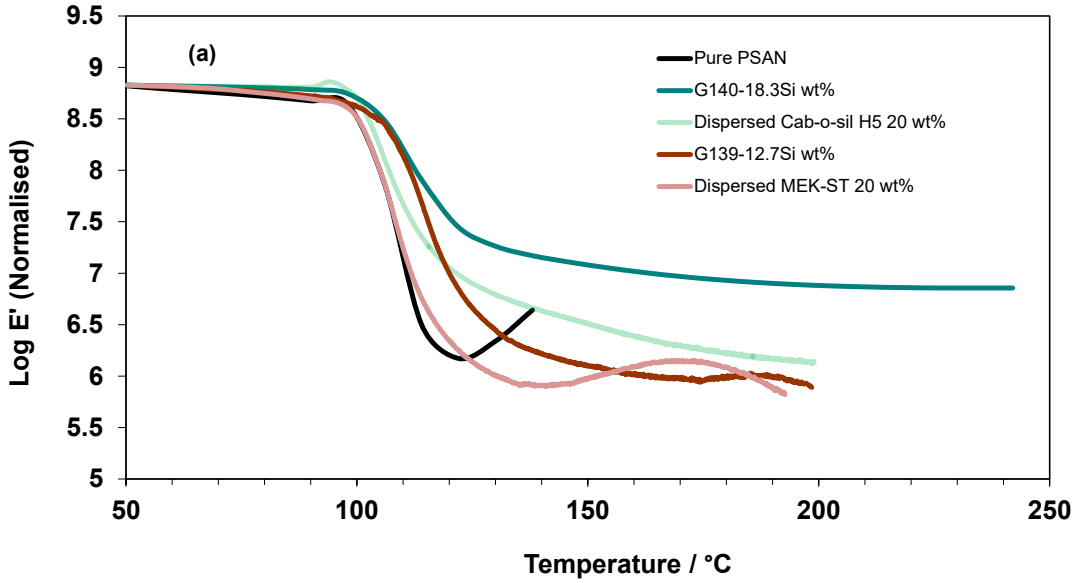

Fig. 5. Plot of normalised storage modulus for PSAN, two dispersed PSAN/silica nanocomposites containing 20wt%silica, and two grafted-PSAN/silica nanocomposites.

4. Conclusion

SAN copolymers were synthesised by AGET ATRP from the surface of functionalised aggregated silica as well as of colloidally dispersed silica nanoparticles using Me_6TREN/Cu(II) as the catalyst, and an organic-soluble tin salt as reducing agent. Silica nanoparticles were found to significantly lower the high-temperature damping in PSAN–silica nanocomposites, at temperatures well (i.e. more than 100 °C) above the T_g of PSAN. The increase in the rubbery modulus was accompanied by the formation of a temperature-independent plateau of the modulus between 130 and 240 °C. While neat PSAN started to flow and deform irreversibly above about 120 °C, the new silica nanoparticle–polymer hybrid materials maintain their dimensional stability up to 250 °C. For these materials, the improvement in dynamic mechanical properties is similar to that of crosslinked polymers and provides clear evidence for suppression of polymer flow. These results suggest the possibility to develop mechanically reinforced hybrid materials and composites with customized mechanical property profiles at elevated temperatures using cheap silica nanoparticles. Future studies need to exploit the applicability of this concept to other polymers, as well as focus on the influence of different types and shapes of silica nanoparticles.

References

[1] Kuan, H.T.N.; Tan, M.Y.; Shen, Y. and Yahya, M.Y. Mechanical properties of particulate organic natural filler-reinforced polymer composite: A review. Composites and Advanced Materials. (2021), 30, p.2634.

[2] Wang, M.J.; Wolff, S. and Tan, E.H. Filler-elastomer interactions. Part VIII. The role of the distance between filler aggregates in the dynamic properties of filled vulcanizates. Rubber chemistry and technology. (1993), 66(2), pp.178-195.

[3] Schaefer, D.W. and Justice, R.S. How nano are nanocomposites? Macromolecules, (2007), 40(24), pp.8501-8517.

[4] Prucker, O. and Rühe, J. Mechanism of radical chain polymerizations initiated by azo compounds covalently bound to the surface of spherical particles. Macromolecules. (1998), 31(3), pp.602-613.

[5] Rühe, J. January. Polymers grafted from solid surfaces. In Macromolecular Symposia. (1998), 126, (1), pp. 215-222). Basel: Hüthig & Wepf Verlag.

[6] Zhang, Z.; Sèbe, G.; Hou, Y.; Wang, J.; Huang, J. and Zhou, G. Grafting polymers from cellulose nanocrystals via surface-initiated atom transfer radical polymerization. Journal of Applied Polymer Science. (2021), 138(48), p.51458.

[7] Eskandari, P.; Abousalman-Rezvani, Z.; Roghani-Mamaqani, H.; Salami-Kalajahi, M. and Mardani, H. Polymer grafting on graphene layers by controlled radical polymerization. Advances in Colloid and Interface Science. (2019), 273, p.102021.

[8] Lacerda, P.S.; Gama, N.; Freire, C.S.; Silvestre, A.J. and Barros-Timmons, A. Grafting poly (methyl methacrylate)(PMMA) from cork via atom transfer radical polymerization (ATRP) towards higher quality of three-dimensional (3D) printed PMMA/Cork-g-PMMA materials. Polymers. (2020), 12(9), p.1867.

[9] Matyjaszewski, K. Advanced materials by atom transfer radical polymerization. Advanced Materials. (2018), 30(23), p.1706441.

[10] Vivek, A.V. and Dhamodharan, R. Grafting of methacrylates and styrene on to polystyrene backbone via a "grafting from" ATRP process at ambient temperature. Journal of Polymer Science Part A: Polymer Chemistry. (2007), 45(17), pp.3818-3832.

[11] Pyun, J.; Jia, S.; Kowalewski, T.; Patterson, G.D. and Matyjaszewski, K. Synthesis and characterization of organic/inorganic hybrid nanoparticles: kinetics of surface-initiated atom transfer radical polymerization and morphology of hybrid nanoparticle ultrathin films. Macromolecules, (2003), 36(14), pp.5094-5104.

[12] Liu, C.H. and Pan, C.Y. Grafting polystyrene onto silica nanoparticles via RAFT polymerization. Polymer. (2007),48(13), pp.3679-3685.

[13] Li, S.; Han, G. and Zhang, W. Photoregulated reversible addition–fragmentation chain transfer (RAFT) polymerization. Polymer Chemistry. (2020), 11(11), pp.1830-1844.

[14] Moad, G. A critical survey of dithiocarbamate reversible addition-fragmentation chain transfer (RAFT) agents in radical polymerization. Journal of Polymer Science Part A: Polymer Chemistry.(2019**)**, 57(3), pp.216-227.

[15] Tsagaropoulos, G.; Eisenberg, A. Dynamic mechanical study of the factors affecting the two glass tranistion behavior of filled polymers . Macromolecules. (1995), 28, 396–398.

[16] Arrighi, V.; McEwen, I. J.; Qian, H.; Serrano Prieto, M. B. The glass transition and interfacial layer in styrene-butadiene rubber containing silica nanofiller. Polymer (2003), 44, 6259–6266.

[17] Yeong, Suk Choi, Mingzhe, Xu. Synthesis of exfoliated poly(styrene-co-acrylonitrile) copolymer/silicate nanocomposite by emulsion polymerization; monomer composition effect on morphology. Polymer (2003), 44, 6989–6994.

[18] Ko, M. Effects of acrylonitrile content on the properties of clay-dispersed poly(styrene-co-acrylonitrile) copolymer nanocomposite. Polymer Bulletin. (2000), 45, 183–190.

[19] Vivek, G.; Tirtha, C.; Lindsay, B; ombalski, Y.; Krzysztof, M.; Ramanan, K.Viscoelastic properties of silica-grafted poly(styrene–acrylonitrile) nanocomposites. Polym Sci Part B: Polym Phys.(2006),44,2014–2023.

[20] Queffelec, J.; Gaynor, S.G.; Matyjaszewski, K. Optimization of atom transfer radical polymerization using Cu(I)/tris(2-(dimethylamino)ethyl)amine as a Catalyst. Macromolecules, (2000), 33, 8629.

[21] Antoni, P.; Nyström, D.; Malmström, E.; Johansson, M.; Hult, A. Synthesis of polystyrene grafting filler nanoparticles, Polym. Prepr. , (2005), 46(1), 477.

[22] Victoria A.; Hans W.; Horn, Gavin O.; Jones, E.; Robert, D. Synthesis of diblock copolymers by combination of organocatalyzed ring-opening polymerization and atom transfer radical polymerization using trichloroethanol as a bifunctional initiator. J. Polym. Sci., Part A: Polym. Chem. (2016), 54, 563–569.

[23] Khlifa, M.; Youssef, A.; Zaed, F.; Kraft, A.; Arrigh, V. Synthesis of polystyrene grafting filler nanoparticles: effect of grafting on mechanical reinforcement. International Journal of chemical and molecular engineering,(2014),8,12

[24] Ohno,K.; Morinaga,T.; Koh. K.; Tsujii, Y.; Fukuda,T. Synthesis of monodisperse silica particles coated with well-defined, high-density polymer brushes by surface-initiated atom transfer radical polymerization. Macromolecules, (2005), 38, 2137.

[25] Li, M.; Min, K.; and Matyjaszewski, K. Simultaneous Reverse & Normal ATRP (SR&NI). Macromolecules. (2004), 37, 2106-2112.

[26] Ojha, S.; Hui, C. M.; Matyjaszewski, K.; and Bockstaller, M. R. Grafting PMMA brushes from α-alumina nanoparticles via SI-ATRP. Mater. Interfaces, (2016), 8 (8), 5458–5465.

[27] Dong, H.; Tang, W. and Matyjaszewski, K. Kinetics of Atom Transfer radical polymerisation. Macromolecules. (2007), 40, 2974-2977.

[28] akubowski, W.; and Matyjaszewski, K. Activator Generated by Electron Transfer for Atom Transfer Radical Polymerisation. Macromolecules (2015), 38, 4139-4146.

[29] Pietrasik, J.; Dong, H.; Matyjaszewski, K. Synthesis of high molecular weight poly(styrene-co-acrylonitrile) copolymers with controlled architecture. Macromolecules, (2006), 39, 6384.

[30] Ha, M. L. P.; Grady, B.P.; Lolli, G.; Resasco, D. E.; Ford, W. T. Composites of single-walled carbon nanotubes and styrene-isoprene copolymer. Macromol. Chem. Phys. (2007), 208, 446–456.

[31] Sugimoto, H.; Daimatsu, K.; Nakanishi, E.; Ogasawara, Y.; Yasumura, T.; Inomata, K. Preparation and properties of poly(methylmethacrylate)–silica hybrid materials incorporating reactive silica nanoparticles. Polymer (2006), 47, 3754–3759.